OXFORD

SOT | Society of Toxicology
academic.oup.com/toxsci

TOXICOLOGICAL SCIENCES, 186(1), 2022, 118–133

https://doi.org/10.1093/toxsci/kfab151
Advance Access Publication Date: 20 December 2021
Research article

Integrated Omic Analyses Identify Pathways and Transcriptomic Regulators Associated With Chemical Alterations of *In Vitro* Neural Network Formation

Carmen A. Marable,[*,†,1] Christopher L. Frank,[*,2] Roland F. Seim,[‡,§,3] Susan Hester,[¶] W. Matthew Henderson,[§] Brian Chorley,[‖] and Timothy J. Shafer[*,4]

[*]Rapid Assay Development Branch, Biomolecular and Computational Toxicology Division, Center for Computational Toxicology and Exposure, U.S. Environmental Protection Agency, Research Triangle Park, North Carolina 27711, USA, [†]Oak Ridge Institute for Science and Education, U.S. Environmental Protection Agency, Research Triangle Park, North Carolina 27711, USA, [‡]Oak Ridge Institute for Science and Education, U.S. Environmental Protection Agency, Athens, Georgia 30605, USA, [§]Chemical Processes and Systems Branch, Center for Environmental Measurement and Modeling, U.S. Environmental Protection Agency, Athens, Georgia 30605, USA, [¶]Experimental Toxicokinetics and Exposure Branch, Chemical Characterization and Exposure Division, Center for Computational Toxicology, U.S. Environmental Protection Agency, Research Triangle Park, North Carolina 27711, USA and [‖]Advanced Experimental Toxicology Models Branch, Biomolecular and Computational Toxicology Division, Center for Computational Toxicology and Exposure, U.S. Environmental Protection Agency, Research Triangle Park, North Carolina 27711, USA

[1]Present address: Curriculum in Neuroscience, University of North Carolina at Chapel Hill, Chapel Hill, NC 27599-7320, USA.

[2]Present address: Verge Genomics, 2 Tower Place, Suite 950, South San Francisco, CA 94080, USA.

[3]Present address: Biological and Biomedical Science Program, University of North Carolina at Chapel Hill, Chapel Hill, NC 27599-7108, USA.

Preparation of this document has been funded by the U.S. Environmental Protection Agency, including a Pathway Innovations Project award to C.L.F. and T.J.S. This document has been subjected to review by the Center for Computational Toxicology and Exposure and approved for publication. Approval does not signify that the contents reflect the views of the Agency, nor does mention of trade names or commercial products constitute endorsement or recommendation for use.

[4]To whom correspondence should be addressed at Rapid Assay Development Branch, Biomolecular and Computational Toxicology Division, Center for Computational Toxicology and Exposure, U.S. Environmental Protection Agency, MD105-05, Research Triangle Park, NC 27711, USA. E-mail: shafer.tim@epa.gov.

ABSTRACT

Development of *in vitro* new approach methodologies has been driven by the need for developmental neurotoxicity (DNT) hazard data on thousands of chemicals. The network formation assay characterizes DNT hazard based on changes in network formation but provides no mechanistic information. This study investigated nervous system signaling pathways and upstream physiological regulators underlying chemically induced neural network dysfunction. Rat primary cortical neural networks grown on microelectrode arrays were exposed for 12 days *in vitro* to cytosine arabinoside, 5-fluorouracil, domoic acid, cypermethrin, deltamethrin, or haloperidol as these exposures altered network formation in previous studies. RNA-seq from cells and gas chromatography/mass spectrometry analysis of media extracts collected on days *in vitro* 12

provided gene expression and metabolomic identification, respectively. The integration of differentially expressed genes and metabolites for each neurotoxicant was analyzed using ingenuity pathway analysis. All 6 compounds altered gene expression that linked to developmental disorders and neurological diseases. Other enriched canonical pathways overlapped among compounds of the same class; eg, genes and metabolites altered by both cytosine arabinoside and 5-fluorouracil exposures are enriched in axonal guidance pathways. Integrated analysis of upstream regulators was heterogeneous across compounds, but identified several transcriptomic regulators including CREB1, SOX2, NOTCH1, and PRODH. These results demonstrate that changes in network formation are accompanied by transcriptomic and metabolomic changes and that different classes of compounds produce differing responses. This approach can enhance information obtained from new approach methodologies and contribute to the identification and development of adverse outcome pathways associated with DNT.

Key words: adverse outcome pathway; developmental neurotoxicity; environmental chemicals; metabolomics; omics research; neural network formation.

Over the last decade, there have been several important legal and/or policy decisions that have encouraged the development and use of *in vitro* approaches for identification of hazard associated with chemical exposure. These include legislative changes such as the REACH act in Europe (European Commission, 2006) and the Lautenberg Chemical Safety Act (United States, 2015) in the United States, and policy decisions such as the 2019 U.S. Environmental Protection Agency memo announcing the intention to develop a new approach methodologies (NAMs) workplan supporting the increased development and implementation of NAMs (Wheeler, 2019). These policy changes have in part been driven by the recognition that for some hazards, data on large numbers of chemicals are lacking, and the use of animal-based testing strategies is insufficient to address this data gap. Further, there is scientific recognition that, for a variety of reasons, animal-based toxicity studies often do not predict adverse outcomes in humans (NRC, 2007). As such, in the last 15 years, there have been significant efforts directed towards the development and implementation of *in vitro* approaches for hazard assessment.

Assessment of developmental neurotoxicity (DNT) hazard has relied heavily on animal-based protocols (EPA 870.6300 [U.S. EPA, 1998] and OECD TG 426 [OECD, 2007]) that assess numerous morphological and behavioral endpoints in offspring exposed, typically perinatally, to chemicals. However, a number of shortcomings of *in vivo* DNT guideline studies have been identified (Tohyama, 2016; Tsuji and Crofton, 2012), including the high cost of conducting the study (approximately $1M/chemical), the large number of animals used (approximately 1000/study), and the amount of time it takes to conduct a DNT guideline study (up to 2 years). One review found that only 15 of 69 guideline DNT studies were used to set points of departure for risk assessments (Raffaele *et al.*, 2010), whereas another review indicated that the learning and memory endpoints evaluated in the guideline DNT studies lack sensitivity (Vorhees and Makris, 2015). Further, these studies do not provide any mechanistic information regarding how a chemical may cause developmental neurotoxicity. Finally, because guideline DNT studies are "triggered" by other evidence of neurotoxicity under the Federal Insecticide, Fungicide and Rodenticide Act, and not at all required under the Toxic Substances Control Act, only a small fraction of chemicals used in the environment have been assessed for DNT (Crofton *et al.*, 2012; Judson *et al.*, 2009). Because of the large number of compounds for which no DNT hazard data are available, there is international agreement that novel approaches to DNT assessment, including *in vitro* screening approaches will be required in order to address this backlog, as current approaches are no longer sufficient (Fritsche *et al.*, 2018).

The lack of data regarding the potential DNT hazard of thousands of compounds in commerce, coupled with the limitations DNT guideline studies discussed above has driven efforts to develop alternative assays for characterizing this hazard. Because development of the nervous system is complex, with multiple potential targets being expressed in different locations and at different times during development, a battery of *in vitro* assays has been proposed as a viable approach to assessing DNT hazard (Bal-Price *et al.*, 2018). This battery consists of phenotypic assays that evaluate key neurodevelopmental processes such as neural progenitor cell proliferation and differentiation, neuronal and glial migration and differentiation, neurite outgrowth and synaptogenesis, and network formation (Bal-Price *et al.*, 2018). This battery of assays consists of both animal (rodent) and human cell models. Although these assays are economical and efficient, they provide only limited information on potential mechanisms by which chemicals may be disrupting these critical neurodevelopmental processes. Information from these *in vitro* assays can be used in Integrated Approaches to Testing and Assessment to inform weight of evidence, fit-for-purpose, screening-level, and/or other regulatory decision scenarios (Paparella *et al.*, 2020). The data from these *in vitro* assays can provide clues for the development of a more formalized framework by providing biological context to reduce the uncertainty of *in vitro* to *in vivo* extrapolation and ultimately lead to the development of possible mechanistic insights associated with DNT (Carlson et al., 2020). Such approaches may inform the development of adverse outcome pathways (AOPs, Watanabe *et al.*, 2011) for developmental neurotoxicity, which are currently lacking (Bal-Price *et al.*, 2015; Sachana et al., 2018).

To address this data gap, this study was conducted as a proof-of-concept, by examining transcriptomic and metabolomic responses following exposure to 6 reference chemicals using rat cortical cultures in a multiplexed format as part of the rodent neural network formation assay (NFA; Brown *et al.*, 2016; Frank *et al.*, 2017)). The NFA evaluates chemical effects on formation of functional networks of rodent neurons grown on microelectrode arrays (MEAs) from days *in vitro* (DIV) 0 to 12. To date, this assay has been used to evaluate the potential DNT of over 200 unique compounds (Brown *et al.*, 2016; Frank *et al.*, 2017; Shafer, 2019). It has high sensitivity and specificity (Shafer, 2019), and has been proposed as a component of the *in vitro* DNT assay battery (Bal-Price *et al.*, 2018). The NFA collects multiple parameters describing chemical effects on the ontogeny of general activity, bursting activity, and coordinated

network activity as well as viability (see Table 2 in Brown *et al.*, 2016). These measures are multiplexed and, due to the noninvasive nature of MEA recordings, collected at 4 different time points during *in vitro* network development. This latter characteristic allows for the determination of toxicological "tipping points" (Frank *et al.*, 2018; Shah *et al.*, 2016), that demark when network development departs from normal trajectories. In this study, developing neural networks were exposed to concentrations of 6 chemicals and electrophysiological data were collected as previously described (Brown *et al.*, 2016). At the end of exposure, media and cell lysates were immediately collected for metabolomic and transcriptomic analyses, respectively, in order to test the hypothesis that a combined -omic analysis would identify pathways, biomarkers, and/or critical genes that were altered by chemical exposure at concentrations that are known to alter neural network development. Such information could help to identify putative AOPs (Bal-Price *et al.*, 2015; Sachana *et al.*, 2018; Watanabe *et al.*, 2011) by identifying relationships between key events (KEs) at the cellular and molecular level and linking them to the KE of altered network formation.

MATERIALS AND METHODS

All data files and scripts supporting this publication are available at DOI: 10.23719/1520859.

Rat primary cortical cultures. Primary neocortical cultures were prepared from postnatal day 0 Long-Evans rat pups. All animal care and tissue harvesting procedures were approved in advance by the U.S. EPA, National Health and Environmental Effects Research Laboratory Institutional Animal Care and Use Committee. Detailed methods for the culture and plating density of cells used for this study have been previously described (Brown *et al.*, 2016; Mundy and Freudenrich, 2000; Valdivia *et al.*, 2014). Cortical cells were plated at a density of 150 000 cells per well on 48-well MEA plates (Axion M768-KAP-48) precoated with 0.05% polyethylenimine. Cells were placed in each well via a 25 µl media drop containing 20 ng/ml (Sigma-Aldrich, Cat No. L2020) laminin administered directly onto the MEA. Two hours after plating cells, 475 µl Neurobasal A media (Gibco, Cat No. 10888022) supplemented with B-27 (Gibco, Cat No. 17504044) was added to each well.

Compounds and dosing. This study evaluated 6 compounds (Table 1) on 48-well MEA plates, all of which have evidence in the literature of DNT effects in humans or mammalian models (Mundy *et al.*, 2015). The screening approaches used for this evaluation (Malo *et al.* 2006) tested each of the 6 selected "proof-of-concept" compounds a minimum of 2 times (Brown *et al.*, 2016; Frank *et al.*, 2017), each time using 3 different MEA plates from the same culture. Thus, each compound has been tested previously with 2 biological replicates consisting of 3 technical replicates each. Compounds (purity >95%) were stored as specified by the manufacturer (Table 1) and were prepared as previously described (Frank *et al.*, 2017; Table 1). Briefly, a stock concentration of 30 mM was prepared and serially diluted by half-log increments to 1000× (between 0.03 and 10 mM) the desired final concentration, then diluted in-well on the 48-well MEA plate 2 h after cell attachment to make a 1× exposure solution (between 0.03 and 10 µM) with solvent maintained at 0.1% (vol/vol). Although all compounds were tested over the entire exposure range used in Frank *et al.* (2017), only selected concentrations were used for transcriptomic and metabolomic analysis due to limited resources for transcriptomic sample analysis. Solvent control wells containing dimethylsulfoxide or H_2O were included to monitor the normal development of cortical cells at final concentrations of 0.1% (vol/vol) and had no effect on network function (Brown *et al.*, 2016). After dosing, the MEAs were

Table 1. Compounds Tested

Compound Name (Abbreviation)	Proposed Target	CAS No.	DTXSID	**Tipping Point**[a] **(µM [±95% CI])**	Concentrations Tested (µM)	**Min Viability**[b] **EC_{50} (µM)**	Solvent Used	Source
Cytosine arabinoside (CA)	DNA synthesis inhibitor	147-94-4	DTXSID3022877	0.046 [0.04–0.06]	1	0.84	DMSO	Sigma-Aldrich
5-Fluorouracil (5FU)	DNA synthesis inhibitor	51-21-8	DTXSID2020634	0.14 [0.10–0.17]	1	2.28	DMSO	Sigma-Aldrich
Domoic acid (DA)	Glutamate Receptor Agonist	14277-97-5	DTXSID20274180	0.21 [0.9–0.25]	0.3	NA	Water	Sigma-Aldrich
Cypermethrin (CM)	Voltage-gated Sodium Channel Modulator	52315-07-8	DTXSID1023998	0.28 [0.19–0.38]	3.10	NA	DMSO	Chem Service, Inc.
Deltamethrin (DM)	Voltage-gated Sodium Channel Modulator	52918-63-5	DTXSID8020381	0.05 [0.04–0.15]	3.10	NA	DMSO	Chem Service, Inc.
Haloperidol (HP)	Dopamine Receptor Agonist	52-86-8	DTXSID4034150	0.31 [0.15–0.49]	3	13.9	DMSO	Sigma-Aldrich

The table shows compound common name, CAS number, DTXSID identifier, the reported tipping point concentration, and the 95% confidence limits, concentrations tested in this study, minimum EC_{50} values for viability (NA = less than 50% cytotoxicity was observed at the highest concentration tested, thus, no EC_{50} value was determined), solvent used for dilutions, and compound source. The DTXSID identifier allows linking the compound to the Computational Toxicology Dashboard (https://comptox.epa.gov/dashboard; last accessed January 5, 2022), which provides further information on structure and other chemical properties.

Abbreviation: DMSO, dimethylsulfoxide.

[a]Frank *et al.* (2017).

[b]Frank *et al.* (2018).

returned to the incubator. After MEA recordings on DIV 5 and 9, the cells received a full media exchange with reexposure to the test compound.

Electrophysiology recordings. A 15-min period of spontaneous network activity was recorded from each well on DIV 5, 7, 9, and 12 using a Maestro 768-channel amplifier, Middle-man data acquisition interface, and Axion Integrated Studio (AxIS) software v2.0 or later (Axion Biosystems, Atlanta, Georgia). Spontaneous activity was measured using a gain of 1200× and a sampling frequency of 12.5 kHz. The signal was filtered through a Butterworth band-pass filter (0.1–5000 Hz) prior to measuring online spike detection (threshold = 8× RMS noise) using the AxIS adaptive spike detector. All recordings were conducted at 37°C with 5% CO_2. Generally, root mean square (RMS) noise on each electrode was between 2 and 5 μV; electrodes with RMS noise exceeding 5 μV were grounded and excluded from recordings.

Normalizing area under the curve values from the MEA plates. The normalized area under the curve (AUC) values for each compound, concentration, and endpoint were determined. The data used for activity were taken from the same cultures that were selected for sequencing and metabolomics. The AUC values were calculated as the trapezoidal AUC from DIV 2 to DIV 12 for each endpoint value from each well. The AUC values were normalized by dividing by the median AUC value of controls on the corresponding MEA plate (see Frank *et al*., 2017).

Metabolomic sample extraction, derivatization, and gas chromatography/mass spectrometry analyses. Following the final DIV 12 MEA recording session, media samples were collected. A volume of 450 μl of media per well was transferred to prelabeled 1.5 ml centrifuge tubes and biological reactions quenched with 50 μl of acetone aliquoted into each tube on ice. The samples were then transferred to the −80°C freezer prior to gas chromatography/mass spectrometry (GC/MS) analyses. Media samples (either test or control) were thawed at room temperature for 1 h and metabolites were simultaneously extracted and derivatized for GC/MS analysis based on the methods of Tao *et al*. (2008). The organic layer was transferred to GC vials for analysis. GC/MS analyses were conducted on an Agilent 6890 GC interfaced to 5973 MS. Sample extracts were analyzed under full-scan (m/z 50-650), electron ionization-MS conditions.

Multivariate statistical analysis of metabolomic samples. Following data collection, each individual chromatogram was exported as netcdf (.AIA) files. All files were imported into Metalign (Lommen, 2009) for spectral preprocessing and alignment following the developer's guidelines for an Agilent GC/MS. Data were then filtered and truncated following the methods of Niu *et al*. (2014). Multivariate statistical analysis was performed by importing Excel spreadsheets of filtered chromatograms into Metaboanalyst (www.metaboanalyst.ca). Preliminary principal component analysis (PCA) was conducted for the entire dataset following Pareto scaled bins to test for outliers. The relative impact of a given chemical exposure was assessed by comparing score values for different treatment classes within a given PCA model. To make these comparisons, the score values for a given component (eg, PC1 scores in a PCA model) were tested for normality using the Kolmogorov-Smirnov test. If found normal, then a 1-way ANOVA test, with Tukey's *post hoc* comparison, was conducted. This allowed the determination of significantly different means (95% confidence) of score values for different treatment classes. All statistical tests on score values were performed with Minitab 16 (Minitab, Inc., State College, Pennsylvania). Statistical significance was ascribed to score values with a p value $< .05$.

Univariate statistical analysis of metabolomics. To determine the significance of metabolite changes resulting from the exposures, volcano plot analysis was conducted with Metabolanalyst coupling fold change (± 1.8) and t test (p value $\leq .05$) analyses. Spectral features identified using this approach were putatively identified using commercially available mass-spectral databases. (Supplementary Figs. 1–4).

Isolation of RNA and sequencing. Total RNA was collected using the Qiagen RNeasy Plus Kit. Two to three wells of identically treated cultures were pooled, representing 1 sample. The experiment was repeated on 2 separate cultures. Samples were pooled by serially treating identically treated wells with a volume of 350 μl of lysis buffer with β-mercaptoethanol (Buffer RLT, Qiagen). This volume was added (as described in RNeasy Plus Kit instructions) to a well and mixed for complete lysis before being transferred to the next (identically treated) well(s) to be pooled together. The lysate sample of pooled wells was transferred to a clean 1.5 ml RNase-free plastic tube and the homogenized lysate sample was then taken through the gDNA Eliminator spin column, and RNA was then precipitated and eluted as described in the RNeasy Plus Kit instructions. The Qubit RNA BR (Broad-Range) Assay Kit was used to measure RNA concentration on the Qubit Fluorometer. Samples were stored in a −80°C freezer until transfer to the NHEERL Genomics Research Core for sequencing. 500 ng total RNA was loaded onto an Apollo 324 automated liquid handler to prepare polyA-selected RNA-seq libraries following manufacturer instructions for a PrepX PolyA mRNA isolation kit (Wafergen). mRNA libraries were denatured with NaOH and loaded onto an Illumina NextSeq 500 bench top sequencer at a final dilution of 1.8 pM with 5% PhiX. Reads were delivered in FastQ file format at an average coverage depth of 15.8 (range = 11.0–23.1) reads per sample.

Analyzing sequences. The sequencer output data files (FASTQ files) were "trimmed" to remove sequence adapters and other low-quality bases from the ends of reads in Partek Flow (Build v4.0.16.0128, St Louis, Missouri). Read ends were trimmed by quality (Q-scores ≤ 7) and reads with length ≤ 25 or composed of any 1 base at $> 95\%$ frequency were removed by Partek Flow. The files were inspected for pre-alignment and postalignment quality control. The sequence was then aligned to a rat reference genome (Rn6) and transcripts were quantified to the transcriptome (RefSeq) by using Spliced Transcripts Alignment to a Reference (STAR) software (STAR2.4.1d, Illumina). Inspection of the postalignment QC metrics was conducted, the reads were mapped to the transcriptome to determine which genes the sequence represents, and annotation (gene level) was completed in the Partek Flow software. Transcript (gene) abundance levels from reads aligned to a rat genome were quantified using expectation-maximization algorithm (E/M) and normalized by dividing by counts per million (CPM) for the sample, adding 1 to all raw counts, and then $\log_2$ transforming. After normalization, a batch effect due to different sequencing runs, which separated rep 1 from reps 2 and 3, was observed. To remove this effect, a general linear model was applied within the Partek Flow environment. Finally, differentially expressed genes (DEGs) were identified using the default Partek Gene-Specific Analysis

algorithm on pairwise groups (control vs treated) followed by pathway mapping with statistical significance which was ascribed to score values with a false discovery rate (FDR) value $<$ 0.05 and absolute fold change value of $\geq$ 2.0. No additional models were enabled to lognormally fit the data.

Integrated omic analysis. To analyze both the metabolomic and the transcriptomic data, a combination of 2 supervised approaches was used within ingenuity pathway analysis (IPA; Qiagen; see Figure 1). First, an independent analysis of both genes and metabolites was conducted. DEG gene lists (1.8$\pm$ fold; p value $<$ .05) peak metabolite lists ($\pm$ 1.8 fold; p value $<$ .05) were also uploaded to IPA and mapped to pathways independently of each other for each compound. Second, following the independent core analysis for each compound, a combined list of genes and metabolites was created for each compound. Utilizing the canonical pathway and upstream regulator analysis functions in IPA, these lists were evaluated for canonical pathway enrichment and potential transcription factor regulators relative to neuronal development. It should be noted that for deltamethrin (DM) and cypermethrin (CM), different treatment concentrations were analyzed for transcriptomics and metabolomics due to a clerical error. As insufficient sample and resources were available to repeat the analysis, the results of the combined analysis used the available data. For independent and integrated analyses, IPA automatically detected entrez IDs for the transcriptomic data using the rodent database and the metabolomic data using the human metabolome database. In both approaches, we focused our analysis to tissues and cells specific to the nervous system, as well as human mapped pathways. Nervous system-related pathways and regulators included select IPA pathway categories like Neurotransmitters and Other

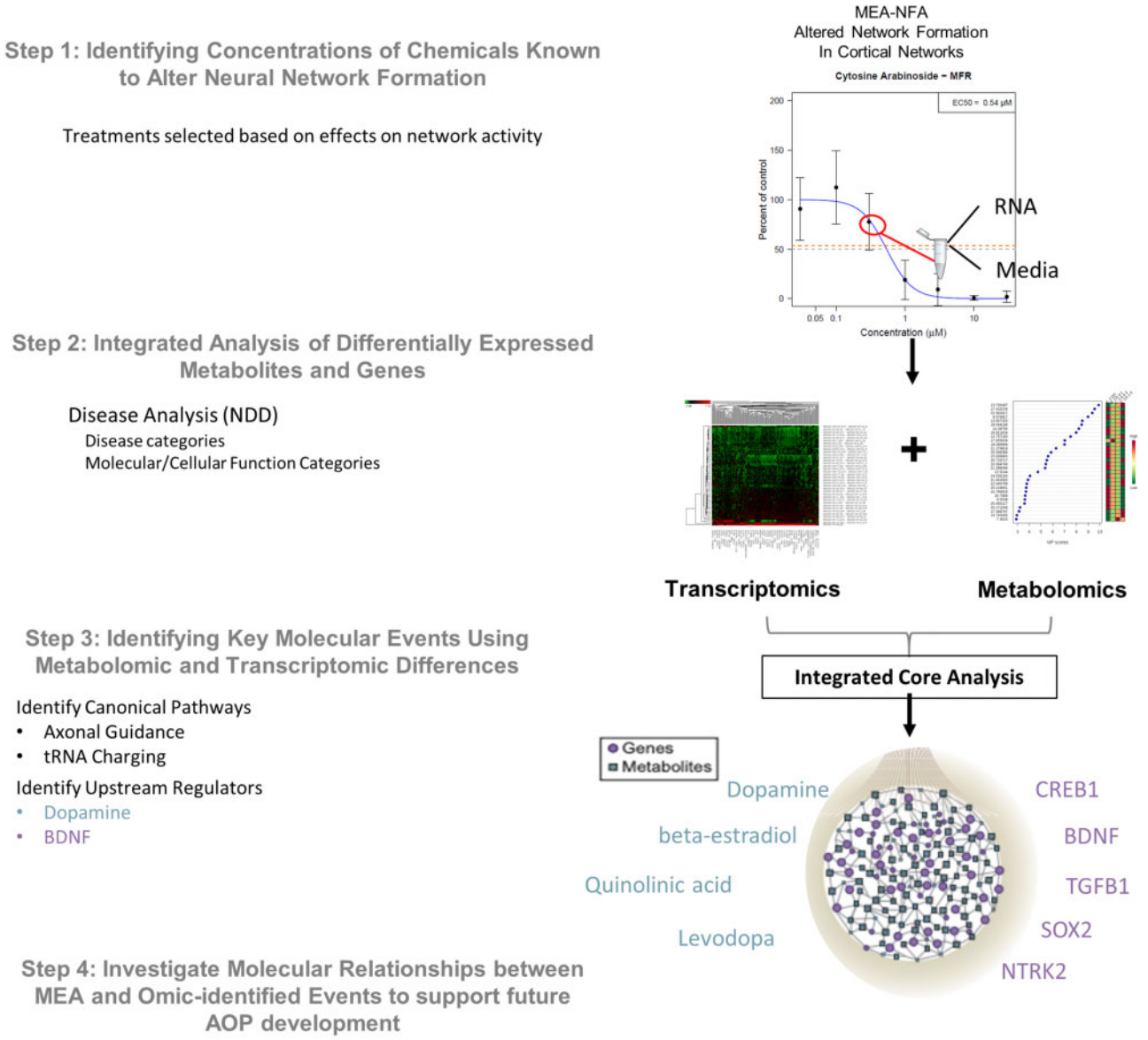

Figure 1. Experimental approach. Chemical concentrations for primary rat cortical cell treatment were selected based on network activity during microelectrode array-network formation assay. The media was used for metabolomic peak identification and RNA was extracted from the plated cells for transcriptomic analysis. Differentially expressed genes and metabolites were assessed independently and then secondarily in an integrated analysis for the 6 chemicals. Key molecular events were identified via ingenuity pathway analysis and were further investigated to determine relatedness in support of future putative adverse outcome pathway development.

Nervous System Signaling, Organismal Growth and Development, Intracellular and Second Messenger Signaling, Growth Factor Signaling, Cytokine Signaling, Cellular Growth, Proliferation and Development, Cell Cycle Regulation, and Disease Specific. These nervous system-related pathway categories were defined by low p values ($< .05$) and large magnitude absolute changes in z-score relative to the significance threshold. Fisher's Exact test p value was used to find the probability that the combined gene, metabolite list would coincide with the IPA pathway list. Upstream analysis function of potential regulators of our lists was based on the number of differentially expressed downstream genes and metabolites in the list and quantified using a Z-score and p value. The Z-score is a correlation measure of how consistently the direction of expression changes in the gene metabolite list matches the direction of change from the annotated literature for targets in the regulatory or biological group.

RESULTS

The overall approach to this study is depicted in Figure 1. Following treatment of developing cortical neuronal networks with chemicals that previously were shown to alter network development (Brown *et al.*, 2016; Frank *et al.*, 2017), RNA was isolated from the cell pellet for transcriptomic analysis and media was saved for metabolomic analysis (Figure 1, step 1). At the highest level, we used IPA to probe neurodevelopmental disease (NDD) Categories associated with the responses to chemical treatment that resulted in altered network development. Separate transcriptomic and metabolomic, as well as integrated analyses were conducted (Figure 1, step 2). The results of analyses were then utilized to identify canonical pathways and upstream regulators associated with altered neuronal network formation following compound exposure (Figure 1, step 3). Last, we investigated the molecular relationships identified between the MEA and multi-omic analyses to provide information on the mechanisms underlying disruption of the neurodevelopmental process (Figure 1, step 4).

Compounds Disrupt Neuronal Network Formation at the Selected Concentrations

The compounds tested in this study were selected based on previous activity in the NFA (Brown *et al.*, 2016), and the concentrations tested in this study are shown (Table 1) relative to their toxicological tipping point (Frank *et al.*, 2018) and EC_{50} value for cytotoxicity (Frank *et al.* 2017); these range from near the cytotoxicity EC_{50} (cytosine arabinoside [CA] and 5 fluorouracil [5FU]) to intermediate between these concentrations (DM/CM/haloperidol [HP]) to near the tipping point concentration (domoic acid [DA]). The toxicological tipping point is the concentration at which network development no longer exhibits recovery from perturbations caused by chemical treatment (ie, homeostasis can no longer compensate for toxicological responses; Frank *et al.*, 2018; Shah *et al.*, 2016). Concentrations were chosen to fall between tipping point and cytotoxicity EC_{50}, as representative of network dysfunction before overt cell death. AUC values for 17 parameters of network formation (eg, mean firing rate, burst rate, interburst interval [IBI], network bursts, etc.) were altered by treatment with all 6 compounds (Figure 2). Overall, most, but not all parameters of network function were reduced by treatment, and distinct profiles of activity are evident across the different treatments. As these effects were generally consistent with previous results (Brown *et al.*, 2016; Frank *et al.*, 2017), no statistical analysis was conducted. Not surprisingly, CA, which was tested at a concentration near its EC_{50} value for cytotoxicity produced the most robust changes (all decreases) in network function across the most network parameters. Interestingly, 5FU, which was also tested near its EC_{50} value for cytotoxicity caused more modest changes in network parameters. Although changes induced by DM, CM, and HP were not as pronounced as for the DNA-synthesis inhibitors, there were clear patterns of response, and in the cases of the pyrethroids (DM and CM), showed concentration-dependence as well as a similarity in the profile of effects on network parameters. For example, CM and DM at the lower concentrations exhibited slight increases in IBI and interspike interval in network spikes (ISNetSP) and to a lesser extent, interspike interval (ISI), whereas HP depressed all parameters except for the percentage of spikes in network spikes (%SpNetSP). In contrast, DA, which was tested at a concentration close to its tipping point, showed small effects on the network function parameters, with the largest effect being an approximately 50% decrease in mutual information (MutInfo).

These changes are consistent with effects previously demonstrated (Brown *et al.*, 2016; Frank *et al.*, 2017) for these compounds on metrics of neural network formation following exposure for 12 DIV. Following the recordings on DIV 12, media samples were collected for metabolomic analysis, and RNA was collected from cell lysates for transcriptomic analysis.

Identification of DEGs Corresponds to the Magnitude of Effects on Network Activity

Table 2 presents the number of identified DEGs associated with nervous tissue for each compound. The number of DEGs generally correlated with the magnitude of chemical effects on network function: 1572 and 304 genes were differentially expressed following treatment with DNA synthesis inhibitors CA and 5FU, respectively. These treatments also caused the most robust alterations in network formation (Figure 2). Although functional changes following DA treatment were subtle, 30 DEGs were identified following treatment with this glutamate receptor agonist. A total of 8 and 10 DEGs were identified following treatment with voltage-gated sodium channel (VGSC) modulators CM and DM, respectively, and 11 following treatment with the dopamine receptor antagonist HP.

Univariate Statistical Analysis Provides an Untargeted Approach to Identify Metabolites

Both PCA and partial least squares discriminant analysis (PLS-DA) were performed in MetaboAnalyst, to identify outliers and allow visualization of each compound by chemical class, respectively. The PLS-DA models showed concentration-dependent class separation. These metabolites were then identified by a Student's t test ($p \leq .05$) comparison across each concentration compared with solvent matched controls tested as described earlier.

Transcriptomic, Metabolomic, and Combined Analyses Identify Molecular and Cellular Function and NDD Categories Associated With Functional Alterations in Network Development

Treatment with the 6 compounds used here resulted in different transcriptomic and metabolomic profiles (Figure 3). The IPA disease analysis tool of Ingenuity identified functional annotations for both DEGs and metabolites, and the integration of genes and metabolites, providing 3 major characterizations. The identified cellular and molecular events were classified by molecular and cellular function, and diseases and disorders, representing 2 hierarchical levels of biology from high levels (diseases and disorders) to molecular levels to aid in translation of results. These characterizations were captured for each

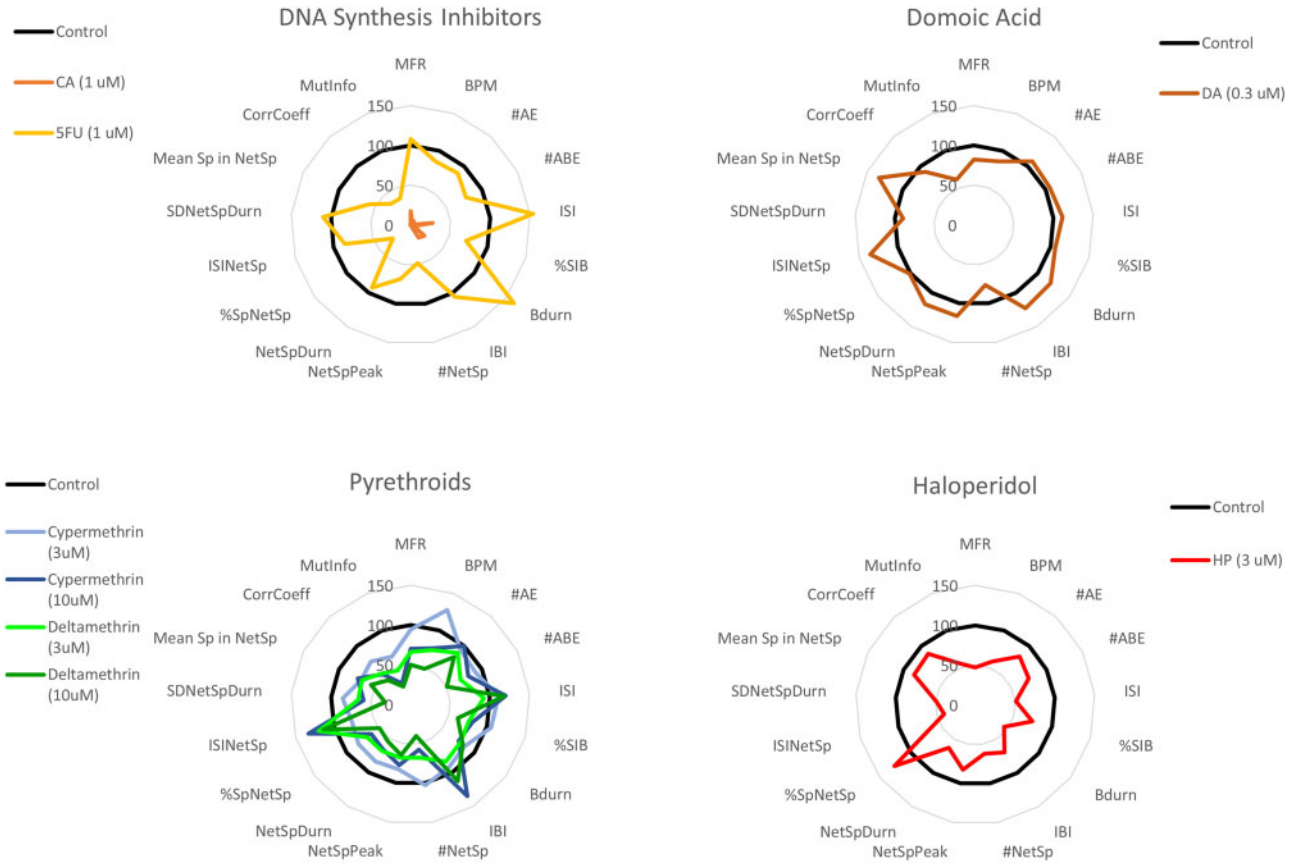

Figure 2. Effects of compounds on network formation. Radar plots of the effects of the 6 compounds tested on neuronal network formation in rat primary cortical cultures. The DNA synthesis inhibitors cytosine arabinoside and 5-fluorouricil are plotted together as are the voltage-gated sodium channel modulators cypermethrin and deltamethrin. In each plot, the different parameters of network development are arranged around the perimeter of the plot, with the center of the plot being zero. The area under the curve for each parameter was determined as described in Frank *et al.* (2017), and is plotted as a percent of control from wells on the same MEA plate. As one proceeds around the plot in a clockwise direction, the parameters evaluate overall activity (MFR- #ABE), then bursting activity (ISI-IBI), Network spiking activity (#NetSp-Mean Sp in NetSp) and finally measures of connectivity (CorrCoeff and MutInfo). Abbreviations: MFR, Mean Firing Rate; BPM, Bursts per Minute; #AE, number of Active Electrodes; #ABE, number of Bursting Electrodes; ISI, interspike interval in a burst; %SIB, percent of spikes that are in a burst; Bdurn, burst duration; IBI, interburst interval; #NetSp, number of network spikes; NetSpPeak, Network Spike Peak; NetSpDurn, network spike duration; %SpNetSP, percent of spikes that are in a network spike; SDNetSpDurn, standard deviation of network spike duration; MeanSp in NetSp, mean number of spikes in network spike; CorrCoeff, correlation coefficient (r); MutInfo, normalized mutual information. See Brown *et al.* (2016) for additional details about network parameters. There are $n = 7–10$ replicates for each treatment/dose group.

Table 2. Differently Expressed Genes (DEGs) and Significant Metabolites

Compound	No. DEGs (14103; 14034 Mapped)	Total No. Metabolites
Cytosine arabinoside (CA)	1572	16
5-Fluorouricil (5FU)	304	17
Cypermethrin (CM)	8	6
Deltamethrin (DM)	10	5
Haloperidol (HP)	11	13
Domoic Acid (DA)	30	14

DEGs and metabolite counts after applying nervous tissue filter in IPA when selecting tissue and cell line settings for the expression analysis.

compound relative to their metabolomic, transcriptomic, and integrated responses inclusive of both transcriptomic and metabolomic data entry. Because CA produced both the most robust changes in DEGs and metabolites, the presentation of results will focus on this exposure as an example and compare and contrast effects of the other compounds to CA. The analyses of all compounds are available in the Supplementary Materials.

Transcriptomic analysis in IPA identified 5 cellular and molecular functions that were associated with CA exposure during network development; cell death and survival, cell morphology, cell growth and proliferation, cellular development, and cellular movement (Figure 4). Like the transcriptomic analysis, metabolomic analysis also identified cellular growth and proliferation. However, the metabolomic analysis identified cell-to-cell signaling and interaction, amino acid metabolism, drug metabolism, and molecular transport. When transcriptomic and metabolomic information were combined, this analysis identified cellular development, cellular movement, cellular growth and proliferation, cell morphology, and cell death and survival as molecular and cellular pathways altered by CA.

The cellular and molecular functions and disease categories that were associated with treatment for the remaining 5 compounds had a high degree of overlap (Figure 4) with those identified for CA. In the combined analysis, cell-to-cell signaling and interaction was identified for 4 compounds (CM, DM, HP, and DA), while cell morphology (CA, CM, and DM), cell death and survival (CA, 5FU, and CM), and cell function and maintenance (5FU, DM, and HP) were each associated with 3 compounds.

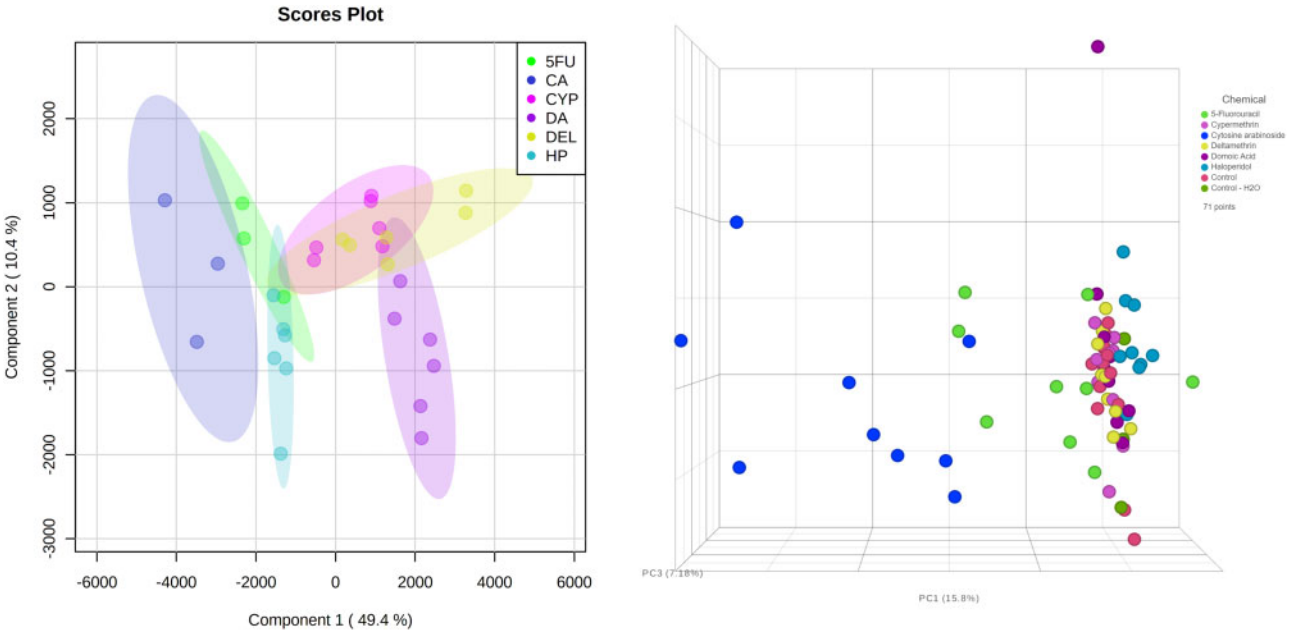

Figure 3. Clustering of each compound by chemical class. Principal component analysis (PCA) show concentration-dependent class separation of identified metabolites (left) and DEGs (right). Each data point represents the average response of solvent matched control cells subtracted from the individual response of exposed cells for each chemical. Note clear separation of treatment groups. See legend on each panel for compound identification.

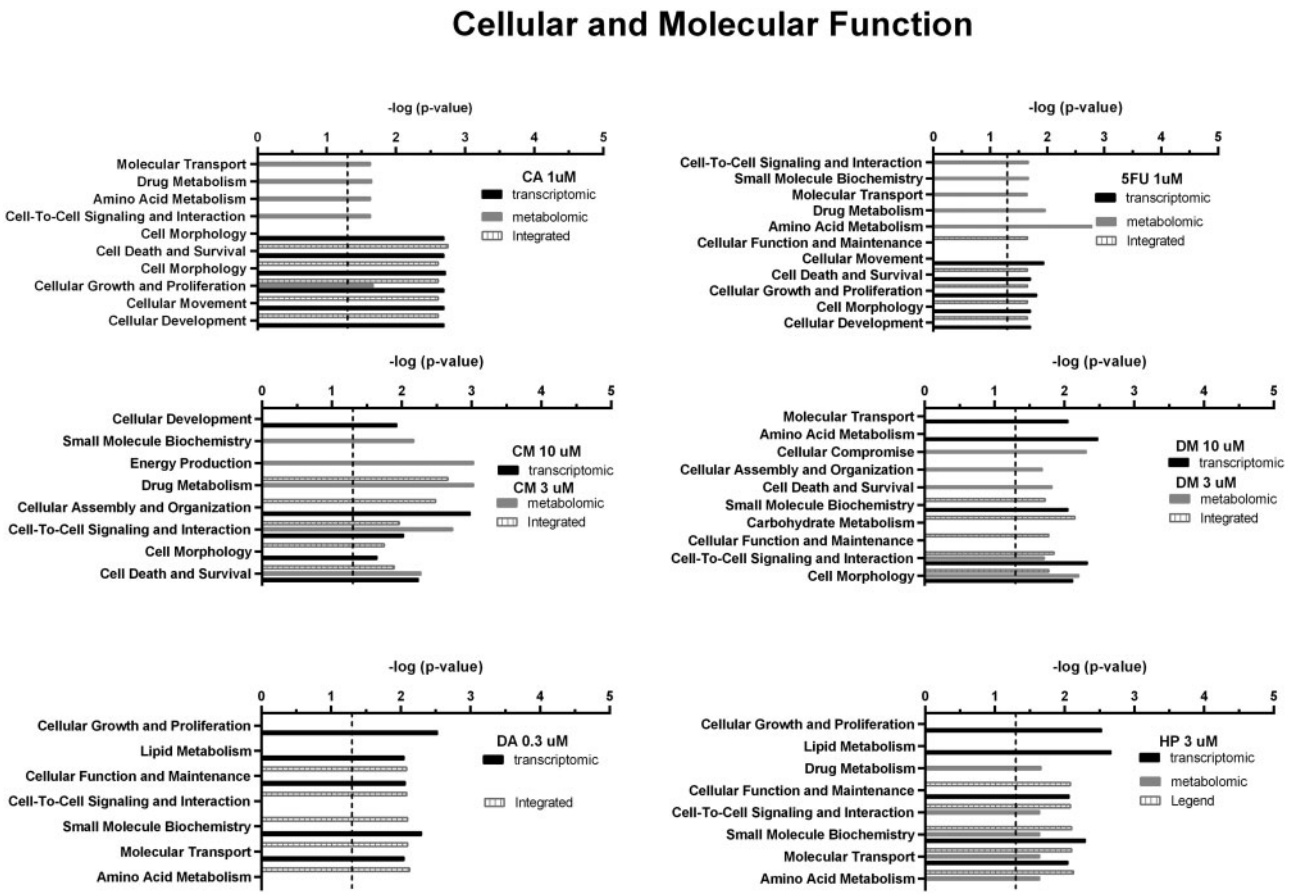

Figure 4. Results of transcriptomic, metabolomic, and combined analyses of cellular and molecular function categories. Statistically significant molecular and cellular function categories resulting from transcriptomic, metabolomic, and combined analysis following exposure to the indicated compounds that disrupt network formation. A common set of 5 disease and disorder categories were altered by the compounds. Values shown are the −log (*p* values), whereas the vertical dotted line represents the level of significance ($p < .05$).

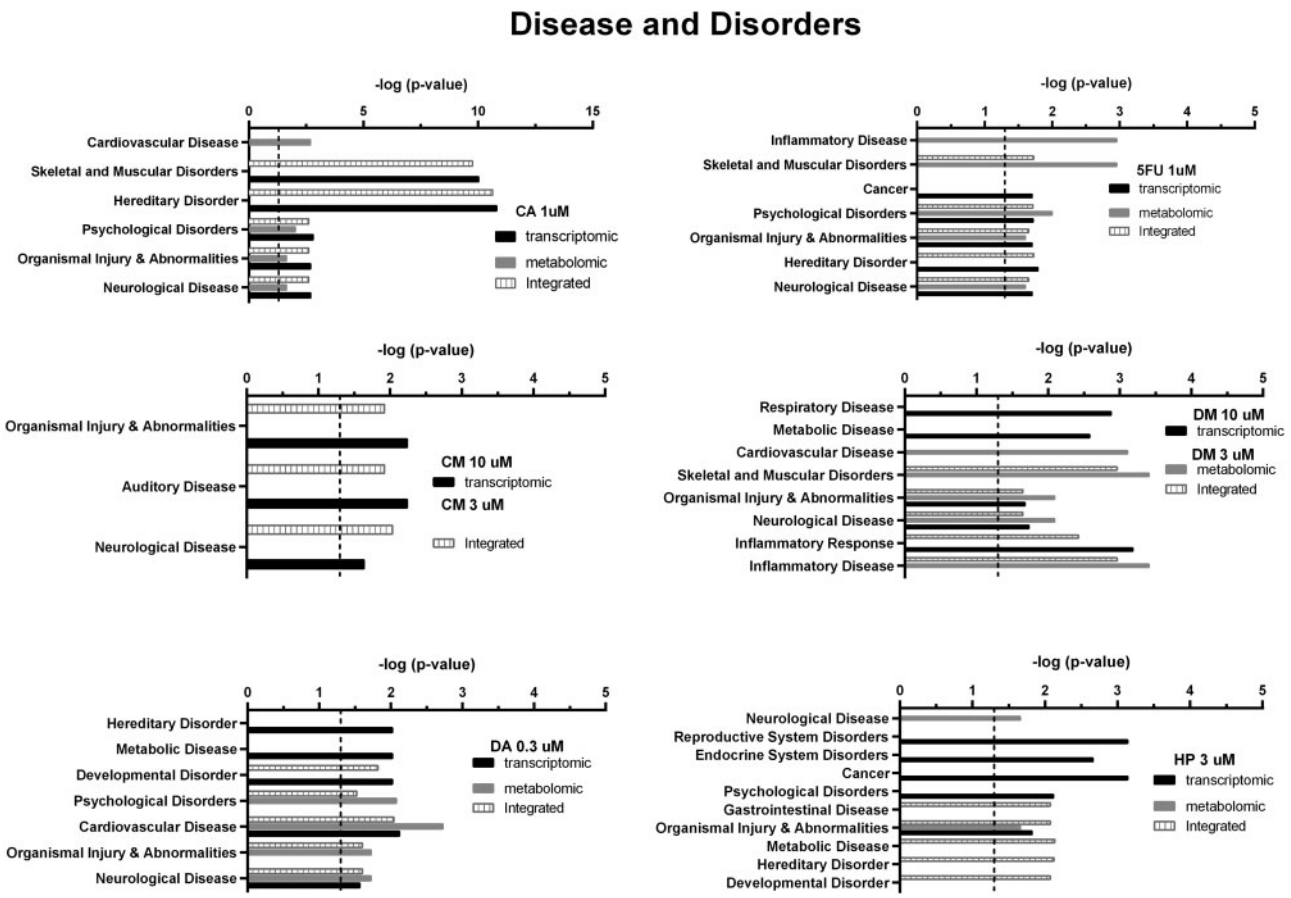

Figure 5. Results of transcriptomic, metabolomic, and combined analyses of disease and disorder categories. Statistically significant disease and disorder categories resulting from transcriptomic, metabolomic, and combined analysis following exposure to the indicated compounds that disrupt network formation. A common set of 5 disease and disorder categories were altered by the compounds. Values shown are the −log (*p* values), whereas the vertical-dotted line represents the level of significance ($p < .05$).

When examining NDD categories associated with the transcriptomic and metabolomic responses to CA, transcriptomic responses identified 5 categories; neurological diseases, organismal injury and abnormality, psychological disorders, hereditary disorders, and skeletal and muscle disorders, whereas the metabolomic responses identified 3 of these 5 (neurological disease, psychological disorders, and organismal injury and abnormality) and the additional category of cardiovascular disease (Figure 5). In the combined analysis the disease categories of neurological disease, organismal injury and abnormalities, psychological disorders, hereditary disorders, and skeletal and muscle disorders were significant (Bonferroni's test, $p < .05$; Figure 5). These categories were prevalent across all compounds in the combined analysis; with all 5 identified for 5FU, 3/5 for DM and DA, and 2/5 for CM and HP (Figure 5). Organismal injury and abnormalities were identified for all 6 compounds, whereas neurological disease was identified for 5/6 compounds (DA being the exception) and psychological disorder for 3/6 (CA, 5FU, and DA).

Identification of Canonical Pathways Altered Following Exposure

Our analysis identified 5 canonical pathways associated with CA: CREB signaling in neurons, axonal guidance signaling, human embryonic stem cell pluripotency, hepatic fibrosis/hepatic stellate cell activation, and osteoarthritis pathway. It is at the level of canonical pathways that even more divergence is observed between the compounds tested (Table 3). The only pathway common between CA and 5FU was axonal guidance signaling (Figure 6). In contrast, this pathway was not among the top pathways identified for the remaining 4 compounds, but tRNA charging was common among these 4 chemicals and 5FU. DA, CM, DM, and HP were associated with several different biosynthesis and degradation pathways, although none of them were common across all 4 of these compounds (Table 3).

Identification of Upstream Regulators Following Exposure

Analysis of upstream regulators for the test chemicals revealed both common regulators as well as regulators unique to each compound (Table 4). SOX2 was common to both CA and 5FU. Although LOC102724788/PRODH was common to CM and DA, otherwise, each compound had different profiles of upstream regulators. All of the identified upstream regulators have important roles in neurodevelopment, as indicated in Tables 5 and 6.

DISCUSSION

This study demonstrates that a multi-omic approach can identify critical pathways involved in neurodevelopment *in vivo* at concentrations of compounds that induce changes in network formation *in vitro*. Exposure to different compound classes during *in vitro* network formation for 12 days resulted in different patterns of effect on network parameters. Further, different

Table 3. Canonical Pathways Associated With Altered Network Formation Using Integrated Pathway Analysis

Cytosine Arabinoside (CA)	5-Fluorouracil (5FU)	Domoic Acid (DA)	Cypermethrin (CM)	Deltamethrin (DM)	Haloperidol (HP)
• CREB signaling in neurons • Axonal guidance signaling • Osteoarthritis pathway • Human embryonic stem cell pluripotency • Hepatic fibrosis/ hepatic stellate cell activation	• WNT/β-catenin signaling • Axonal guidance signaling • tRNA charging • Hepatocyte Growth Factor (HGF) signaling • Nicotinamide adenine dinucleotide (NAD) signaling pathway • Hepatic fibrosis/ hepatic stellate cell activation	• tRNA charging • Phenylalanine degradation IV (mammalian, via side chain) • Glycine biosynthesis III • Purine nucleotides de novo biosynthesis II • Tyrosine biosynthesis IV	• Alanine biosynthesis III • Glycine biosynthesis III • Catecholamine biosynthesis • tRNA charging • Glycine Biosynthesis III • Thio-molybdenum cofactor biosynthesis	• (S)-reticuline biosynthesis II • Tyrosine degradation I • 4-hydroxybenzoate biosynthesis • 4-hydroxyphenylpyruvate biosynthesis • tRNA charging	• Phenylalanine degradation I • Threonine degradation II • Tyrosine biosynthesis IV • Glycine biosynthesis III • tRNA charging

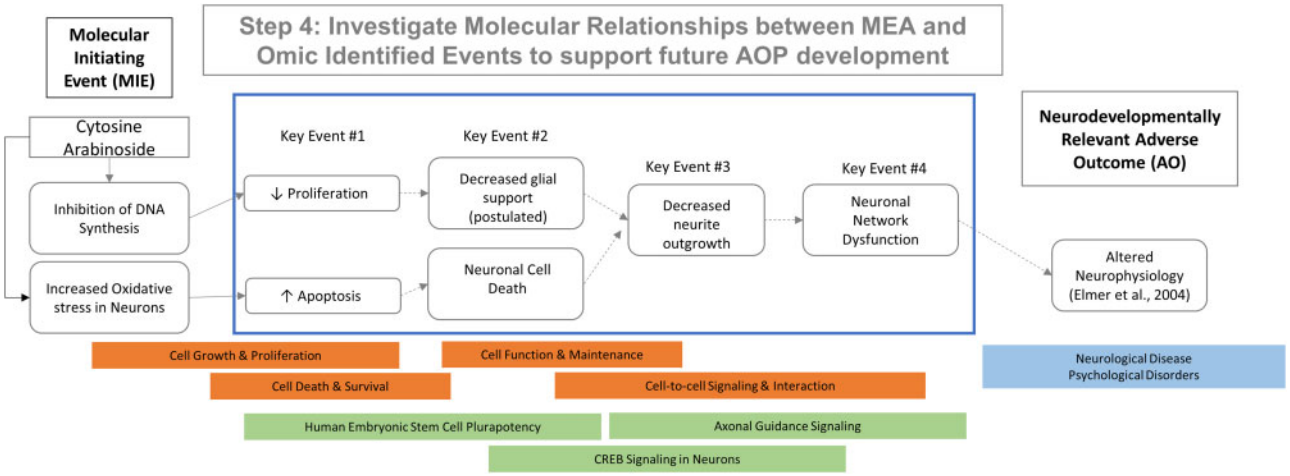

Figure 6. Putative adverse outcome pathway linked to cytosine arabinoside exposure. Illustrated here is a putative adverse outcome pathway (AOP) for altered neurophysiology that is based on data (blue outline) from the microelectrode array network formation assay as well as other *in vitro* developmental neurotoxicity assays (see Harrill *et al.*, 2018) after cytosine arabinoside exposure. Underneath the putative AOP are the cellular and molecular categories (orange), disease and disorder categories (light blue), and canonical pathways (light green) that were identified by -omic approaches following treatment with cytosine arabinoside. Overlap of the orange and light green bars is approximate. Key event relationships that are well established are indicated with solid arrows, while those that are postulated are indicated by dashed arrows.

classes of compounds evoked different -omic responses, with compounds from the same class (eg, CA and 5FU) evoking similar responses while compounds from different classes (eg, DM and HP) evoked differential responses. This result suggests that these compounds are disrupting neural network formation through alteration of different pathways, but potentially with class-specific AOPs.

The need for novel methods to evaluate chemicals for DNT hazard is now well-established. In the last decade, a variety of *in vitro* assays based on the ability of chemicals to disrupt key neurodevelopmental events have been developed. Many of these neurodevelopmental events, such as proliferation, neurite outgrowth, synaptogenesis, etc., can be considered as KEs that could be involved in AOPs for compounds with DNT hazard potential. Among these assays, the neural NFA (Brown *et al.*, 2016; Frank *et al.*, 2017; Shafer, 2019) is unique in that it evaluates neuronal function, rather than structural or molecular endpoints. However, the NFA as currently performed does not provide any mechanistic information. Given that "alterations in network function" are listed as a KE in 5 AOPs found on the AOPWiki (https://aopwiki.org/events/386; last accessed January 5, 2022), understanding in more detail the pathways underlying alterations in network formation can serve to strengthen the existing AOPs involving this KE, and identify additional putative AOPs.

All 6 compounds tested in this study have been reported to cause DNT in mammals (Mundy *et al.*, 2015). At the highest level of organization evaluated in this study (NDD), all 6 compounds were associated with a highly common set of categories for both cellular and molecular function as well as disease and development disorders (Figs. 4 and 5). The categories were consistent across the transcriptomic, metabolomic, and combined analyses, indicating common and robust responses to compound treatment. This information establishes an important linkage from the *in vitro* work conducted here to *in vivo*, human adverse neurodevelopmental outcomes by demonstrating that the -omic changes induced *in vitro* are disrupting some of the same processes that result in human NDD states. It is important to note that we are not postulating that exposure to these

Table 4. Top Upstream Regulators Associated with Chemical Exposures That Alter Network Formation

	Cytosine Arabinoside (CA)	5-Fluorouracil (5FU)	Domoic Acid (DA)	Cypermethrin (CM)	Deltamethrin (DM)	Haloperidol (HP)
Transcriptomic regulators	CREB1↑	SOX2↓	LOC102724788/ PRODH	ARX	ATXN1	CREB1
	SOX2↓	TCF7L2↓	SLC1A2	LOC102724788/ PRODH	GLS	CA9
	ZBTB17	PRMT1↓	ELAVL4	SLC1A2	HPRT1	CPT1B
	S100A8↑	PPP3CA	GLS	KLF9	ELAVL4	
		NOTCH1		SLC23A2		
Metabolomic regulators	β-estradiol		Kynurenic acid		K+	Afatinb
						GSKJ4

Predicted activation (↑) and inhibition (↓). Lack of a directional arrow indicates that activation or inhibition could not be predicted.

chemicals would cause a specific NDD such as (eg) schizophrenia, but rather that some aspects of disrupted neurodevelopment that occur following exposure to these chemicals during development have commonalities with the perturbations that result in NDD states. That chemical disruption of nervous system development and neurodevelopmental diseases has commonalities at the disease and developmental disorder level is not unexpected, nor is it surprising that common cellular and molecular categories were impacted by these chemicals. It is noteworthy that the overall functional response of the networks was also consistent for all compounds, being generally decreased in both the limited analysis in this study, as well as the more complete analyses in previous studies (Brown *et al.*, 2016; Frank *et al.*, 2017). Thus, there is general agreement between the functional and -omic responses at the highest levels.

When examining canonical pathways associated with the alterations in network function; however, some divergence begins to appear between the different classes of compounds. Axonal guidance signaling was associated only with the DNA synthesis inhibitors (CA and 5FU), whereas tRNA charging was common among 5 of the compounds. This could be a result of an integrated stress response (Kapur *et al.*, 2017). Alteration of biosynthesis pathways was a common finding among the remaining 4 compounds (CM, DM, DA, and HP); however, all of the specific pathways identified were unique to each compound. Canonical pathway and upstream regulator identification for each compound may play a role in different KEs of neurodevelopment, which are all essential to formation of neuronal networks (Reiner *et al.*, 2016). A similar theme was identified at the level of upstream regulators associated with compound exposure, with common regulators as well as unique regulators associated with each compound or among compounds with similar mechanisms. SOX2 was common to both of the DNA synthesis inhibitors, whereas LOC102724788/PRODH was common to CM and DA, otherwise the upstream regulators were unique for each compound.

Overall, these results help us build putative AOPs based on the multi-omic responses to compound exposures studied here. At the highest level of organization, they converge upon a common physiological response (decreased activity in network formation patterns) and disease categories (eg, neurological disorders, organismal injury, and abnormalities). As one begins to explore further the canonical pathways contributing to these disease categories, some common pathways are found (eg, axonal guidance), but more importantly different pathways begin to emerge that can be associated with different compound classes and their modes of action. This hypothesis is further supported by the analysis of upstream regulators, which show some commonalities across chemicals, but more broadly identified unique patterns of response for each compound. These results suggest that the actions on network function are the result of not a single AOP contributing to the decrease in activity, but rather a network of AOPs converging to impact physiological function as measured by the MEA. It is likely that decreases in network function following exposure to these compounds are the summation of several different events, such as decreases in neurite outgrowth, synaptogenesis, synaptic support from glia, and even differing levels of cytotoxicity/cell death. Thus, it could be expected that an interconnected AOP network will evolve with additional studies.

This information can then be combined with information from other sources to begin to develop putative AOPs for further exploration (Figure 1, step 4). An online analysis tool DAVID could be used as a complimentary source of interest in future projects to compare and potentially confirm which dysregulated signaling pathways are enriched relative to the IPA identified key upstream regulators and their predicted activation. Both CA and 5FU are known inhibitors of proliferating cells by inhibiting DNA synthesis, CA also causes oxidative stress in neurons (Geller *et al.*, 2001). These may serve as initial KEs, where exposure of the cortical cultures used here results in decreased proliferation of the glial cells and increased oxidative stress in neurons. Further, according to Harrill *et al.* (2018), both CA and 5FU increased apoptosis and decreased proliferation in neuroprogenitor cells, and this also has been reported in primary cultures of cortical neurons (Geller *et al.*, 2001). Neurite outgrowth has also been reported to be decreased by CA (Harrill *et al.*, 2018) at concentrations similar to those used in this study. It has been demonstrated previously that compounds that decrease neurite outgrowth in cortical cells can also decrease network formation (Robinette *et al.*, 2011). These effects on apoptosis, proliferation, and neurite outgrowth were nonselective, indicating that they were associated with loss of cell viability (Harrill *et al.*, 2018). Both CA and 5FU also alter network formation, not only here but also in previous experiments (Brown *et al.*, 2016; Frank *et al.*, 2017). Thus, one can postulate an AOP as illustrated in Figure 6, wherein the actions of CA on neurons and glia in the cortical culture converge on decreased neurite outgrowth and ultimately result in decreased network formation. The different cellular and molecular and disease categories, as well as the canonical pathways can then be overlaid onto the putative AOP. Finally, one can begin to investigate this AOP in a more rigorous manner by manipulating the upstream regulators such as, SOX2, CREB1 (CA), NOTCH1 (5FU), and the other regulators in Table 4 to build confidence in the KE

Table 5. Transcriptomic Upstream Regulators and Their Roles in Neurodevelopment

Upstream Regulator	Gene/Protein Name	Neurodevelopmental Relevance	Reference
ARX	*Aristaless-related homeobox*	ARX is a paired-like transcription factor that serves as an essential regulator in a network of genes needed for normal forebrain patterning and growth	Lim *et al.* (2019)
ATXN1	*Ataxin 1*	Functions as a transcriptional repressor and modulates transcription that disrupts the dopaminergic pathway	Opal (2010)
CA9	*Carbonic Anhydrase 9*	Can influence the function of proton-sensitive membrane proteins involved in neuronal signaling	Ruusuvuori *et al.* (2013)
CREB1	*CAMP Responsive Element Binding Protein 1*	Nuclear transcription factor that regulates neuronal plasticity	Chang *et al.* (2009)
CPT1B	*Carnitine palmitoyltransferase 1B*	Enzyme required for the net transport of long-chain fatty acyl-CoAs and its dysregulation has been found to be a key player involved in neuronal function survival.	Zhang *et al.* (2015)
ELAVL4	*ELAV Like RNA Binding Protein 4*	Regulates the fate of neuronal mRNAs; implicated in neuronal plasticity, namely in recovery from axonal injury, learning and memory, and multiple neurological diseases	Bronicki and Jasmin (2013)
GLS	*Glutaminase*	Plays a role in excitatory synapses and participates in migration, proliferation, and differentiation of neural stem progenitor cells	Benavides-Rivas *et al.* (2020)
HPRT1	*Hypoxanthine Phosphoribosyltransferase 1*	Regulates molecular and cellular functions during neuronal differentiation as well as mechanisms that determine neuronal/glial cell fate decisions during neurogenesis	Kang *et al.* (2013)
KLF9	*Krüppel-like factor 9*	Inhibits neurite outgrowth/axon regeneration and promotes neuronal development/plasticity	Avci *et al.* (2012) and Bonett *et al.* (2009)
LOC102724788/PRODH	*Proline dehydrogenase 2*	Regulates proline catabolism, which is vital for normal Central Nervous System (CNS) functioning; and encodes proline dehydrogenase, which is involved in neuromediator synthesis in the CNS	Suntsova *et al.* (2013)
NOTCH1	*Notch homolog 1*	Inhibits neurite outgrowth in postmitotic primary neurons	Berezovska *et al.* (1999)
PPP3CA	*Protein Phosphatase 3 Catalytic Subunit Alpha*	Essential in the transduction of intracellular Ca^{2+}-mediated signals	Myers *et al.* (2017)
PRMT1	*Protein Arginine Methyltransferase 1*	Significant regulator of glial cell function during postnatal brain development	Hashimoto *et al.* (2021)
SLC1A2	*Solute Carrier Family 1 Member 2*	Essential for glutamatergic neurotransmission	Penadés *et al.* (2020)
SOX2	SRY-Box Transcription Factor 2	Marker of neuroprogenitor status; expression inhibits neuronal differentiation	Graham *et al.* (2003)

Table 5.. (continued)

Upstream Regulator	Gene/Protein Name	Neurodevelopmental Relevance	Reference
SLC23A2	*Solute Carrier Family 23 Member 2*	Transporter that provides high ascorbate concentration in CNS; ascorbate is responsible for myelin formation, protection against glutamate toxicity and synaptic potentiation	May (2012)
S100A8	S100 Calcium Binding Protein A8	An anti-inflammatory protein that contributes to apoptosis and antiproliferation	Passey *et al.* (1999)
TCF7L2	*Transcription Factor 7 Like 2*	Master regulator that regulates different stages of postmitotic differentiation in the thalamus	Lipiec *et al.* (2020)
ZBTB17	*Zinc Finger And BTB Domain Containing 17*	Involved in cell cycle regulation	Lawir *et al.* (2017)

Table 6. Metabolomic Upstream Regulators and Their Roles in Neurodevelopment

Metabolite/Chemical	Neurodevelopmental Relevance	Reference
B-estradiol	Plays a role in the regulation of synaptogenesis	Kretz *et al.* (2004)
Kynurenic acid	Impacts cortical development	Bagasrawala *et al.* (2016)
K+	Essential for neuronal signaling and sphingolipid synthesis; sphingolipids are key players in cell proliferation, differentiation, and transformation	Ferland (2012)
Afatinb	Potent and selective Epidermal Growth Factor Receptor (EGFR)-tyrosine kinase inhibitor; EGFR is differentially expressed in neurons and glia during development and is critical to cell migration, maturation, survival, and proliferation	Chen *et al.* (2019)
GSKJ4	Inhibits cellular proliferation through prompting cell death and by suppressing the cell cycle	Mandal *et al.* (2017)

relationships (KERs) for cell proliferation, survival, neurite outgrowth, and network formation.

Such an approach can be taken for the other compound classes as well. At concentrations similar to those used here, HP was a selective inhibitor of neurite initiation in both hN2 and rat cortical neurons (EC_{30} = approximately 3 μM), and nonselectively inhibited synaptogenesis at higher concentrations (Harrill et al., 2018). Data for DA and CM were not available from Harrill *et al.* (2018). In a recently released report, neither DA nor CM was active in a variety of *in vitro* DNT assays examining neurite outgrowth, proliferation, and glial function, suggesting its actions on network formation are relatively specific (Masjosthusmann *et al.*, 2020). However, in a rat neural stem cell model, DA was reported to reduce the differentiation of stem cells into astrocytes, neurons, and oligodendrocytes at noncytotoxic concentrations (Gill and Kumara, 2019) Further, higher concentrations reduced axonal length (Gill and Kumara, 2019). DM was more selective than some of the other chemicals tested here in that it decreased only neurite maturation and synaptogenesis at concentrations (EC_{30} = approximately 9 μM) that were about twofold below cytotoxicity (Harrill *et al.*, 2018). Putative AOPs for DM, HP, and DA are presented in Supplementary Figures 5–7, respectively. Note that for DA, the level of information regarding potential KEs identifies several important data gaps. All of these putative AOPs require additional investigation and further development. In particular, the levels of evidence for each proposed KE need to be further evaluated and KERs need to be established. However, knowledge of the upstream regulators identified in this study can be leveraged to conduct experiments that inform the KERs.

Several important caveats should be considered with respect to the current dataset. First, the samples for the -omic responses were collected only at the end of the exposure period over which network formation was evaluated with MEAs. Thus, the pathways and regulators identified here may not represent the initial response to perturbation of network development, but rather the downstream consequences of those initial responses. Although metabolomic time-course data could be collected easily by simply collecting media samples over time, collection of a transcriptomic response time-course would require the use of sister cultures such that cells could be lysed and RNA collected at each timepoint. Second, it should be recognized that the primary cortical culture used here is a mixed culture consisting of excitatory and inhibitory neurons as well as glia. Therefore, these individual cell types may respond differently, and obscure the ability to detect an influential response that is not occurring in the majority of cells or in a dominant cell population. Under the protocol used here, it would not be possible to discriminate differential responses of the cell types, and small responses in a single cell type might not be large enough to reach the limits of detection/significance, which could influence the identified pathways. Similarly, the metabolomics analysis was based on media samples, not intracellular metabolites. It is possible that such an approach favored detection of metabolites more associated with cellular death or altered membrane integrity over those that might reflect other

biochemical processes. The advantage of this approach is that it would lend itself to repeated metabolomic analyses over time from the same well/population of cells. Third, the concentrations tested in this study were limited, and covered a different range of responses for the different compounds. DA was tested at the lowest concentration, which was near its toxicological "tipping point" concentration (Frank *et al.*, 2018) where the homeostatic compensatory processes of the cell are overwhelmed. CM, DM, and HP were all tested at 10- to 100-fold higher than their respective tipping points, but were not cytotoxic (CM and DM) or were well below (HP) their cytotoxicity EC_{50} values. In contrast, the DNT synthesis inhibitors were tested at concentrations that were close to or slightly exceeding their EC_{50} values for cytotoxicity. Consequently, these differences may also contribute to the differential responses observed for each compound in the -omic responses. Since few DEGs went into the analysis for CM, DM, and HP, it was more difficult to identify commonly enriched pathways. Finally, the present experiments used primary cultures of rodent neurons, and therefore the results obtained here may not apply directly to humans. Additional studies are needed to resolve these questions, but the present results demonstrate that this approach can identify and support hypotheses regarding the mechanisms underlying alterations in neural network formation that can then be investigated further. Such an approach will provide valuable information for AOP development.

CONCLUSION

This study demonstrates the feasibility of this approach in obtaining -omic information from NFAs that incorporate rodent (or in the future, human) neuronal models. The transcriptomic and metabolomic responses help reinforce the functional MEA observations, suggesting that changes in these pathways may underlie the functional changes. This justifies further studies into the mechanisms of action in rat cortical cells and the relationship of these changes to -omic changes in neurodevelopmental disorders. Future studies could explore which DEGs and/or metabolites are most predictive for network dysfunction.

SUPPLEMENTARY DATA

Supplementary data are available at *Toxicological Sciences* online.

DECLARATION OF CONFLICTING INTERESTS

The authors declared no potential conflicts of interest with respect to the research, authorship, and/or publication of this article.

ACKNOWLEDGMENTS

The authors thank Ms Theresa Freudenrich and Ms Kathleen Wallace for their outstanding technical support with tissue culture on this project. They also greatly appreciate the assistance of Dr Anna Fisher from the EPA's genomics core. Finally, they are grateful the insightful comments on an earlier version of this manuscript from Dr Leah Wehmas (U.S. EPA) and Dr Rebecca Fry (University of North Carolina at Chapel Hill).

REFERENCES

Avci, H. X., Lebrun, C., Wehrlé, R., Doulazmi, M., Chatonnet, F., Morel, M.-P., Ema, M., Vodjdani, G., Sotelo, C., Flamant, F., *et al.* (2012). Thyroid hormone triggers the developmental loss of axonal regenerative capacity via thyroid hormone receptor α1 and Krüppel-like factor 9 in Purkinje cells. *Proc. Natl. Acad. Sci. U.S.A.* **109**, 14206–14211.

Bagasrawala, I., Zecevic, N., and Radonjić, N. V. (2016). N-methyl D-aspartate receptor antagonist kynurenic acid affects human cortical development. *Front. Neurosci.* **10**, 435.

Bal-Price, A., Crofton, K. M., Sachana, M., Shafer, T. J., Behl, M., Forsby, A., Hargreaves, A., Landesmann, B., Lein, P. J., Louisse, J., *et al.* (2015). Putative adverse outcome pathways relevant to neurotoxicity. *Crit. Rev. Toxicol.* **45**, 83–91.

Bal-Price, A., Hogberg, H. T., Crofton, K. M., Daneshian, M., FitzGerald, R. E., Fritsche, E., Heinonen, T., Hougaard Bennekou, S., Klima, S., Piersma, A. H., *et al.* (2018). Recommendation on test readiness criteria for new approach methods in toxicology: Exemplified for developmental neurotoxicity. *ALTEX* **35**, 306–352.

Benavides-Rivas, C., Tovar, L. M., Zúñiga, N., Pinto-Borguero, I., Retamal, C., Yévenes, G. E., Moraga-Cid, G., Fuentealba, J., Guzmán, L., Coddou, C., *et al.* (2020). Altered glutaminase 1 activity during neurulation and its potential implications in neural tube defects. *Front. Pharmacol.* **11**, 900.

Berezovska, O., McLean, P., Knowles, R., Frosh, M., Lu, F. M., Lux, S. E., and Hyman, B. T. (1999). Notch1 inhibits neurite outgrowth in postmitotic primary neurons. *Neuroscience* **93**, 433–439.

Bonett, R. M., Hu, F., Bagamasbad, P., and Denver, R. J. (2009). Stressor and glucocorticoid-dependent induction of the immediate early gene Kruppel-like factor 9: Implications for neural development and plasticity. *Endocrinology* **150**, 1757–1765.

Bronicki, L. M., and Jasmin, B. J. (2013). Emerging complexity of the HuD/ELAVl4 gene; Implications for neuronal development, function, and dysfunction. *RNA* **19**, 1019–1037. doi:10.1261/rna.039164.113

Brown, J. P., Hall, D., Frank, C. L., Wallace, K., Mundy, W. R., and Shafer, T. J. (2016). Editor's highlight: Evaluation of a microelectrode array-based assay for neural network ontogeny using training set chemicals. *Toxicol. Sci.* **154**, 126–139.

Carlson, L. M., Champagne, F. A., Cory-Slechta, D. A., Dishaw, L., Faustman, E., Mundy, W., Segal, D., Sobin, C., Starkey, C., Taylor, M., *et al.* (2020). Potential frameworks to support evaluation of mechanistic data for developmental neurotoxicity outcomes: A symposium report. *Neurotoxicol. Teratol.* **78**, 106865.

Chang, S., Wen, S., Chen, D., and Jin, P. (2009). Small regulatory RNAs in neurodevelopmental disorders. *Hum. Mol. Genet.* **18**, R18–R26.

Chen, Y.-J., Hsu, C.-C., Shiao, Y.-J., Wang, H.-T., Lo, Y.-L., and Lin, A. M. Y. (2019). Anti-inflammatory effect of afatinib (an EGFR-TKI) on OGD-induced neuroinflammation. *Sci. Rep.* **9**, 2516–2516.

Crofton, K. M., Mundy, W. R., and Shafer, T. J. (2012). Developmental neurotoxicity testing: A path forward. *Congenit. Anom. (Kyoto)* **52**, 140–146.

Elmer, G. I., Sydnor, J., Guard, H., Hercher, E., and Vogel, M. W. (2004). Altered prepulse inhibition in rats treated prenatally with the antimitotic Ara-C: An animal model for sensorimotor gating deficits in schizophrenia. *Psychopharmacology (Berl.)*, **174**, 177–189.

European Commission. (2006). EC Regulation (EC) No 1907/2006 of the European Parliament and of the Council of 18 December 2006 concerning the Registration, Evaluation, Authorisation and Restriction of Chemicals (REACH), establishing a European Chemicals Agency, amending Directive 1999/45/EC and repealing Council Regulation (EEC) No 793/93 and Commission Regulation (EC) No 1488/94 as well as Council Directive 76/769/EEC and Commission Directives 91/155/EEC, 93/67/EEC, 93/105/EC and 2000/21/EC, OJ L 396, p. 1. Available at: https://eur-lex.europa.eu/LexUriServ/LexUriServ.do?uri=OJ:L:2007:136:0003:0280:en:PDF. Accessed February 1, 2022.

Ferland, G. (2012). Vitamin K and the nervous system: An overview of its actions. *Adv. Nutr.* **3**, 204–212.

Frank, C. L., Brown, J. P., Wallace, K., Mundy, W. R., and Shafer, T. J. (2017). From the cover: Developmental neurotoxicants disrupt activity in cortical networks on microelectrode arrays: Results of screening 86 compounds during neural network formation. *Toxicol. Sci.* **160**, 121–135. doi:10.1093/toxsci/kfx169

Frank, C. L., Brown, J. P., Wallace, K., Wambaugh, J. F., Shah, I., and Shafer, T. J. (2018). Defining toxicological tipping points in neuronal network development. *Toxicol. Appl. Pharmacol.* **354**, 81–93.

Fritsche, E., Grandjean, P., Crofton, K. M., Aschner, M., Goldberg, A., Heinonen, T., Hessel, E. V. S., Hogberg, H. T., Bennekou, S. H., Lein, P. J., *et al.* (2018). Consensus statement on the need for innovation, transition and implementation of developmental neurotoxicity (DNT) testing for regulatory purposes. *Toxicol. Appl. Pharmacol.* **354**, 3–6.

Geller, H. M., Cheng, K. Y., Goldsmith, N. K., Romero, A. A., Zhang, A. L., Morris, E. J., and Grandison, L. (2001). Oxidative stress mediates neuronal DNA damage and apoptosis in response to cytosine arabinoside. *J. Neurochem.* **78**, 265–275.

Gill, S., and Kumara, V. M. R. (2019). Detecting neurodevelopmental toxicity of domoic acid and ochratoxin a using rat fetal neural stem cells. *Mar. Drugs* **17**, 566.

Graham, V., Khudyakov, J., Ellis, P., and Pevny, L. (2003). SOX2 functions to maintain neural progenitor identity. *Neuron* **39**, 749–765.

Harrill, J. A., Freudenrich, T., Wallace, K., Ball, K., Shafer, T. J., and Mundy, W. R. (2018). Testing for developmental neurotoxicity using a battery of in vitro assays for key cellular events in neurodevelopment. *Toxicol. Appl. Pharmacol.* **354**, 24–39.

Hashimoto, M., Kumabe, A., Kim, J.-D., Murata, K., Sekizar, S., Williams, A., Lu, W., Ishida, J., Nakagawa, T., Endo, M., *et al.* (2021). Loss of PRMT1 in the central nervous system (CNS) induces reactive astrocytes and microglia during postnatal brain development. *J. Neurochem.* **156**, 834–847.

Judson, R., Richard, A., Dix, D. J., Houck, K., Martin, M., Kavlock, R., Dellarco, V., Henry, T., Holderman, T., Sayre, P., *et al.* (2009). The toxicity data landscape for environmental chemicals. *Environ. Health Perspect.* **117**, 685–695.

Kang, T. H., Park, Y., Bader, J. S., and Friedmann, T. (2013). The housekeeping gene hypoxanthine guanine phosphoribosyltransferase (HPRT) regulates multiple developmental and metabolic pathways of murine embryonic stem cell neuronal differentiation. *PLoS One* **8**, e74967.

Kapur, M., Monaghan, C. E., and Ackerman, S. L. (2017). Regulation of mRNA translation in neurons-a matter of life and death. *Neuron* **96**, 616–637.

Kretz, O., Fester, L., Wehrenberg, U., Zhou, L., Brauckmann, S., Zhao, S., Prange-Kiel, J., Naumann, T., Jarry, H., Frotscher, M., *et al.* (2004). Hippocampal synapses depend on hippocampal estrogen synthesis. *J. Neurosci.* **24**, 5913–5921.

Lawir, D.-F., Iwanami, N., Schorpp, M., and Boehm, T. (2017). A missense mutation in zbtb17 blocks the earliest steps of T cell differentiation in zebrafish. *Sci. Rep.* **7**, 44145.

Lim, Y., Cho, I.-T., Shi, X., Grinspan, J. B., Cho, G., and Golden, J. A. (2019). Arx expression suppresses ventralization of the developing dorsal forebrain. *Sci. Rep.* **9**, 226.

Lipiec, M. A., Bem, J., Koziński, K., Chakraborty, C., Urban-Ciećko, J., Zajkowski, T., Dąbrowski, M., Szewczyk, ŁM., Toval, A., Ferran, J. L., *et al.* (2020). TCF7L2 regulates postmitotic differentiation programmes and excitability patterns in the thalamus. *Development* **147**, dev190181.

Lommen, A. (2009). MetAlign: Interface-driven, versatile metabolomics tool for hyphenated full-scan mass spectrometry data preprocessing. *Anal. Chem.* **81**, 3079–3086. doi:10.1021/ac900036d

Malo, N., Hanley, J. A., Cerquozzi, S., Pelletier, J., and Nadon, R. (2006). Statistical practice in high-throughput screening data analysis. *Nat. Biotechnol.* **24**,167–175.

Mandal, C., Kim, S. H., Kang, S. C., Chai, J. C., Lee, Y. S., Jung, K. H., and Chai, Y. G. (2017). GSK-J4-mediated transcriptomic alterations in differentiating embryoid bodies. *Mol. Cells* **40**, 737–751.

Masjosthusmann, S., Blum, J., Bartmann, K., Dolde, X., Holzer, A.-K., Stürzl, L.-C., Keßel, E. H., Förster, N., Dönmez, A., Klose, J., *et al.* (2020). Establishment of an a priori protocol for the implementation and interpretation of an in-vitro testing battery for the assessment of developmental neurotoxicity. *EFSA Support. Publ.* **17**, 1938E.

May, J. M. (2012). Vitamin C transport and its role in the central nervous system. *Subcell Biochem.* **56**, 85–103.

Mundy, W. R., and Freudenrich, T. M. (2000). Sensitivity of immature neurons in culture to metal-induced changes in reactive oxygen species and intracellular free calcium. *Neurotoxicology* **21**,1135–1144.

Mundy, W. R., Padilla, S., Breier, J. M., Crofton, K. M., Gilbert, M. E., Herr, D. W., Jensen, K. F., Radio, N. M., Raffaele, K. C., Schumacher, K., *et al.* (2015). Expanding the test set: Chemicals with potential to disrupt mammalian brain development. *Neurotoxicol. Teratol.* **52**, 25–35. doi:10.1016/j.ntt.2015.10.001

Myers, C. T., Stong, N., Mountier, E. I., Helbig, K. L., Freytag, S., Sullivan, J. E., Ben Zeev, B., Nissenkorn, A., Tzadok, M., Heimer, G., *et al.* (2017). De novo mutations in PPP3CA cause severe neurodevelopmental disease with seizures. *Am. J. Hum. Genet.* **101**, 516–524.

National Research Council. (2007). *Toxicity Testing in the 21st Century: A Vision and a Strategy*. The National Academies Press, Washington, DC. Available at: https://doi.org/10.17226/11970. Accessed February 1, 2022.

Niu, W., Knight, E., Xia, Q., and McGarvey, B. D. (2014). Comparative evaluation of eight software programs for alignment of gas chromatography-mass spectrometry chromatograms in metabolomics experiments. *J. Chromatogr. A* **1374**,199–206.

Organization for Economic Cooperation and Development (OECD). (2007). *OECD Guidelines for the Testing of Chemicals. Section 4: Health Effects*. Test No. 426. Developmental Neurotoxicity Study. Available at: https://www.oecd-ilibrary.org/docserver/9789264067394-en.pdf?expires=1523434361&id=id&accname=ocid84004878&checksum=C46D0BEFDF0D3B6B5BE313A857358BA9. Accessed January 5, 2022.

Opal, P. (2010). Ataxin. In *Encyclopedia of Movement Disorders* (K. Kompoliti and L. V. Metman, Eds.), pp. 94–95. Academic Press, Oxford.

Paparella, M., Bennekou, S. H., and Bal-Price, A. (2020). An analysis of the limitations and uncertainties of in vivo developmental

neurotoxicity testing and assessment to identify the potential for alternative approaches. *Reprod. Toxicol.* **96**, 327–336.

Passey, R. J., Xu, K., Hume, D. A., and Geczy, C. L. (1999). S100A8: Emerging functions and regulation. *J. Leukoc. Biol.* **66**, 549–556.

Penadés, R., Bosia, M., Catalán, R., Spangaro, M., García-Rizo, C., Amoretti, S., Bioque, M., and Bernardo, M. (2020). The role of genetics in cognitive remediation in schizophrenia: A systematic review. *Schizophrenia Res. Cogn.* **19**, 100146.

Raffaele, K. C., Rowland, J., May, B., Makris, S. L., Schumacher, K., and Scarano, L. J. (2010). The use of developmental neurotoxicity data in pesticide risk assessments. *Neurotoxicol. Teratol.* **32**, 563–572.

Reiner, O., Karzbrun, E., Kshirsagar, A., and Kaibuchi, K. (2016). Regulation of neuronal migration, an emerging topic in autism spectrum disorders. *J. Neurochem.* **136**, 440–456.

Robinette, B., Harrill, J., Mundy, W. R., and Shafer, T. J. (2011). In vitro assessment of developmental neurotoxicity: Use of microelectrode arrays to measure functional changes in neuronal network ontogeny. *Front. Neuroeng.* **4**,1.

Ruusuvuori, E., Huebner, A. K., Kirilkin, I., Yukin, A. Y., Blaesse, P., Helmy, M., Kang, H. J., El Muayed, M., Hennings, J. C., Voipio, J., *et al.* (2013). Neuronal carbonic anhydrase VII provides GABAergic excitatory drive to exacerbate febrile seizures. *EMBO J.* **32**, 2275–2286.

Sachana, M., Rolaki, A., and Bal-Price, A. (2018). Development of the Adverse Outcome Pathway (AOP): Chronic binding of antagonist to N-methyl-d-aspartate receptors (NMDARs) during brain development induces impairment of learning and memory abilities of children. *Toxicol. Appl. Pharmacol.* **354**, 153–175.

Shafer, T. J. (2019). Application of microelectrode array approaches to neurotoxicity testing and screening. *Adv. Neurobiol.* **22**, 275–297.

Shah, I., Setzer, R. W., Jack, J., Houck, K. A., Judson, R. S., Knudsen, T. B., Liu, J., Martin, M. T., Reif, D. M., Richard, A. M., *et al.* (2016). Using ToxCast™ data to reconstruct dynamic cell state trajectories and estimate toxicological points of departure. *Environ. Health Perspect.* **124**, 910–919.

Suntsova, M., Gogvadze, E. V., Salozhin, S., Gaifullin, N., Eroshkin, F., Dmitriev, S. E., Martynova, N., Kulikov, K., Malakhova, G., Tukhbatova, G., *et al.* (2013). Human-specific endogenous retroviral insert serves as an enhancer for the schizophrenia-linked gene PRODH. *Proc. Natl. Acad. Sci. U.S.A.* **110**, 19472–19477.

Tao, X., Liu, Y., Wang, Y., Qiu, Y., Lin, J., Zhao, A., Su, M., and Jia, W. (2008). GC-MS with ethyl chloroformate derivatization for comprehensive analysis of metabolites in serum and its application to human uremia. *Anal. Bioanal. Chem.* **391**,2881–2889.

Tohyama, C. (2016). Developmental neurotoxicity test guidelines: Problems and perspectives. *J. Toxicol. Sci.* **41**, SP69–SP79.

Tsuji, R., and Crofton, K. M. (2012). Developmental neurotoxicity guideline study: Issues with methodology, evaluation and regulation. *Congenit. Anom. (Kyoto)* **52**, 122–128.

United States Congress Senate Committee on Environment and Public Works. (2015). Legislative hearing on the Frank R. Lautenberg Chemical Safety for the 21st Century Act (S. 697): Hearing before the Committee on Environment and Public Works, United States Senate, One Hundred Fourteenth Congress, first session, March 18, 2015. U.S. Government Publishing Office. For sale by the Superintendent of Documents, Washington, DC. S hrg.

US Environmental Protection Agency (US EPA). (1998). *Health Effects Guidelines OPPTS 870.6300 Developmental Neurotoxicity Study*. Office of Prevention Pesticides and Toxic Substances. Available at: https://nepis.epa.gov/Exe/ZyPURL.cgi?Dockey=P100G6UI.TXT. Accessed January 5, 2022.

Valdivia, P., Martin, M., LeFew, W. R., Ross, J., Houck, K. A., and Shafer, T. J. (2014). Multi-well microelectrode array recordings detect neuroactivity of ToxCast compounds. *Neurotoxicology* **44**, 204–217.

Vorhees, C. V., and Makris, S. L. (2015). Assessment of learning, memory, and attention in developmental neurotoxicity regulatory studies: Synthesis, commentary, and recommendations. *Neurotoxicol. Teratol.* **52**, 109–115.

Wheeler, A. R. (2019). *Memorandum: Directive to Prioritize Efforts to Reduce Animal Testing*. Available at: https://www.epa.gov/sites/production/files/2019-09/documents/image2019-09-09-231249.pdf. Accessed January 5, 2022.

Zhang, L., Li, H., Hu, X., Benedek, D. M., Fullerton, C. S., Forsten, R. D., Naifeh, J. A., Li, X., Wu, H., Benevides, K. N., *et al.* (2015). Mitochondria-focused gene expression profile reveals common pathways and CPT1B dysregulation in both rodent stress model and human subjects with PTSD. *Transl. Psychiatry* **5**, e580.